
Cascade Centrality with heterogeneous nodal influence in a noisy environment

Yan Leng, Yehonatan Sella and Alex ‘Sandy’ Pentland

MIT Media Lab

{yleng, ysellar, pentland }@mit.edu

Abstract

Centrality is a fundamental building block in network analysis. Existing centrality measures focus on the network topology without considering nodal characteristics. However, this ignorance is perilous if the cascade payoff does not grow monotonically with the size of the cascade. In this paper, we propose a new centrality measure, Cascade Centrality, which integrates network position, the diffusion process, and nodal characteristics. It nests and spans the gap between degree, eigenvector, Katz, and diffusion centrality. Interestingly, when $p\lambda_1 > 1$, eigenvector, Katz and diffusion centrality all collapse to Cascade Centrality with a scaling factor determined by the distribution of eigenvector and the nodal influence vector. Furthermore, the presence of homophily in social networks enables the de-noising of real-world observations. Therefore, we propose a unified framework to simultaneously learn the actual nodal influence vector and network structure with an iterative learning algorithm. Experiments on synthetic and real data show that Cascade Centrality outperforms existing centrality measures in generating cascade payoffs. Moreover, with the proposed algorithm, the de-noised centrality measure is more correlated with the actual Cascade Centrality than merely computing from the observations. Cascade Centrality can capture more complex behaviors and processes in the network and has significant implications for theoretical studies in influence maximization and practical applications in viral marketing and political campaign.

1 Introduction

Over the past decade, there has been a fast-growing number of studies focusing on the connectedness of various aspects of the societies, ranging from the networks of individuals to institutions and industries [14, 18, 1]. Centrality is a fundamental concept in networks. The positioning of individuals in a network drives a wide range of behaviors, such as information diffusions in social networks and cascading failures in financial institutions [1]. Depending on different applications, there are numerous ways to compute an objects’ centrality in a network. For example, degree centrality can describe who is first hit in a contagion [9]. Eigenvector centrality can determine the distribution of incentives to maximize social welfare [10]. Katz centrality determines one’s power in strategic interaction on networks [4]. Diffusion centrality depicts an individual’s role in information diffusion [6].

All these centralities operate similarly and can be represented by a function of the position of nodes in a network [7]. In other words, existing centralities are only related to the topological structure and node’s positioning on the network. Similarly, in the influence maximization literature, started from the seminal paper Kempe, Kleinberg and Éva [15], the objective is to maximize the reach of a cascade, which is only related to the network structure. This objective function, viewing every node contributes positively, carries some nice properties including monotonicity and submodularity [13, 16].

However, overlooking nodal characteristics fails to capture some behaviors and dynamics in numerous applications. The most prominent example is in viral marketing. Several existing studies have witnessed the phenomena that information reaching individuals who review negatively about the product may hurt the campaign, such as sales on Groupon and public announcement on Goodreads and online video platform [8, 17, 2]. Degree centrality, Katz centrality and eigenvector centrality does not work in this context since they only capture one’s ability to diffuse a piece of information to a large number of individuals. These centralities grow monotonically with the cascade size initiated by each individual. In other words, these centrality measures do not capture individuals’ heterogeneous contribution, positively or negatively, to the objective function.

Moreover, most centrality measures treat observed network as deterministic or perfectly observed. However, with the noisy and static data in real life, links between individuals might be unobserved, spurious or lagged-behind [12, 19]. In this scenario, centrality measures based on observed networks may not be robust and reliable. More importantly, noises in the data may be an even more severe concern when we consider the contribution of nodal influence to cascade payoff, which can be positive and negative. We provide an upper bound for the robustness of our centrality measure with observational errors in either nodal influence vector or the network. More practically, we formulate a learning problem to estimate the underlying network and the nodal influence vector in the face of noisy observations. In particular, our approach extends upon lower-rank matrix completion with graph information [3, 22, 22], and further infer the network structure from the noisy observations. To be more specific, to solve the challenge when both nodal characteristics and the networks are imperfectly observed, we formulate a joint optimization problem and an iterative learning algorithm to learn nodal characteristics and the network simultaneously.

The main contributions of this paper are two-fold. First, we propose a new centrality measure, Cascade Centrality, which integrates network position, dynamic process, and the nodal influence to cascade payoff. It extends and generalizes degree, eigenvector, Katz, and diffusion centrality. Interestingly, we show that when $p\lambda_1 > 1$, then eigenvector, diffusion and cascade centralities all collapse to Cascade Centrality with a multiplier. Second, we provide an algorithm to compute Cascade Centrality in a noisy environment by de-noising the nodal influence vector and the network. In this paper, we provide a novel and more general centrality measure to capture more general behaviors in a network in a noisy environment and sheds light on influence maximization literature and other practical applications, such as viral marketing and political campaigns.

2 Setup

Given a set of n individuals $N = 1, \dots, n$, the adjacency matrix of the network is \mathbf{A} , which is an n -by- n symmetric matrix. The entry \mathbf{A}_{ij} equals 1 if there exists a link, and 0 otherwise. Let $\mathbf{D} = \text{diag}(\mathbf{d})$, where $d_i = \sum_{j=1}^n \mathbf{A}_{ij}$ denotes the degree of node i . The Laplacian of the the adjacency matrix \mathbf{A} is $\mathbf{L} = \mathbf{D} - \mathbf{A}$, in which $L_{ij} = d_i - A_{ij}$ if $i \neq j$ and $L_{ij} = d_i$ if $i = j$. We term individual i ’s contribution to the cascade payoff the nodal influence of i , denoted y_i , with the vector of nodal influence represented by $\mathbf{y} \in \mathbb{R}^n$.

The diffusion process in our study follows independent cascade model [15]. In particular, an individual who has a piece of information has a homogeneous probability p to diffuse to his neighbor. The widely adopted objective function in influence maximization is $\sigma = \sum_{i=1}^N \mathbb{P}_i$, with $\mathbb{P} \in \mathbb{R}^{N \times 1}$ representing the probability of individual i receiving the information [15, 23, 20].

In our objective function, rather than treating the activation of any node homogeneously positive, we allow each node’s value to the cascade payoff to vary heterogeneously, rather than increasing monotonically with the size of the cascade. To this end, we let the payoff of the seeder be the overall influence summed over the network cascade. In particular, let r_i be the expected number of times individual i receives the piece of information, for $\mathbf{r} \in \mathbb{R}^n$). Therefore, the cascade payoff σ is the weighted sum of the nodal influence vector \mathbf{y} ,

$$\sigma = \sum_{i=1}^N r_i y_i. \tag{1}$$

With Singular Value Decomposition on the symmetric adjacency matrix, we have $\mathbf{A} = \mathbf{U}\mathbf{\Lambda}\mathbf{U}^T$, where $\mathbf{\Lambda} = \text{diag}\{\mathbf{\Lambda}\} = \{\lambda_1, \lambda_2, \dots, \lambda_n\}$ in a descending order and the corresponding eigenvectors are $\{U_1, U_2, \dots, U_n\}$ with U_1 as the dominant eigenvector.

In this paper, we denote $\text{trace}(\cdot)$, $\|\cdot\|_F$ and $\rho(\cdot)$ as the trace, Frobenius norm and spectral radius of a matrix. Moreover, $\|\cdot\|$ and $\max(\cdot)$ are the Euclidean norm and maximum of a vector.

3 Cascade Centrality

In this section, we introduce Cascade Centrality (CC) and bound it above and below by the network structure and the nodal influence vector. Our centrality measure is a generalization over degree centrality, eigenvector centrality, Katz centrality and diffusion centrality. Furthermore, when $p\lambda_1 > 1$, we provide an approximation to Cascade Centrality as well as eigenvector and diffusion centralities. Under this condition, these centrality measures approximately boil down to a Cascade Centrality with a multiplier. Lastly, we analyze the robustness of Cascade Centrality when observations and measurements of the nodal influence vector and the network are noisy.

3.1 Definition and bounds for Cascade Centrality

Cascade Centrality is a walk-based centrality, weighing the different nodes differently according to the vector \mathbf{y} . The matrix $(p\mathbf{A})^t$ records the expected number of walks of length t from one individual to another. T is the maximum walk length allowed. By varying T , we can flexibly adjust for the measurement of nodal centrality from local (small T) to global (large T). We now present the formal definition of Cascade Centrality.

Definition 1. *Cascade Centrality (CC) is defined as the vector whose i th entry is the expected payoff generated by the network cascade if only individual i is seeded,*

$$CC(\mathbf{A}; p, \mathbf{y}, T) := \sum_{t=0}^T (p\mathbf{A})^t \mathbf{y}. \quad (2)$$

Our centrality measure builds upon the diffusion centrality proposed in by Banerjee, Chandrasekhar, Duflo, and Jackson [5] and is more generalizable. The ranking in Cascade Centrality is the same as that in diffusion centrality if \mathbf{y} is a constant vector, namely, the nodal influence is the same for all nodes. Another slight difference is that when $p = 0$, diffusion centrality scores all individuals equally. However, Cascade centrality coincides with the nodal influence vector \mathbf{y} . Under the condition that \mathbf{y} is constant, our centrality measure inherits the nice nesting property from diffusion centrality, which encompasses and spans the gap between degree centrality, eigenvector centrality, and Katz centrality. It is straightforward to observe that, when \mathbf{y} is constant, (i) CC linearly scales with degree centrality when $T = 1$. (ii) CC is proportional to eigenvector centrality when $T \rightarrow \infty$ and $p \geq \lambda_1^{-1}$. (iii) CC is proportional to Katz centrality when $T \rightarrow \infty$ and $p \leq \lambda_1^{-1}$.

In this section, we study bounds for Cascade Centrality under the assumption that $p\lambda_1 < 1$. The next section examines the case $p\lambda_1 > 1$.

Theorem 1 bounds Cascade Centrality above and below with the network structure and the nodal characteristic vector. It thus provides us with a tool to evaluate the range for the cascade payoff of a given network and the corresponding influence. These bounds have two applications: 1) they facilitate the understanding of the bottleneck for diffusion on a network; 2) they help to select a network from alternatives ones in practical applications to ensure comparatively more substantial cascade payoff, such as more successful marketing campaign. The proof for Theorem 1 can be found in the Appendix.

Theorem 1.

$$(1 + p\lambda_n)\|\mathbf{y}\| \leq \|CC(\mathbf{A}; p, \mathbf{y}, T)\| \leq \frac{1}{1 - p\lambda_1}\|\mathbf{y}\| \quad (3)$$

The maximum value in the vector of Cascade Centrality captures the effectiveness of the campaign with only one seed. We bound $\max(CC)$ in Corollary 1, which are similarly determined by the largest eigenvalue, and the norm of the nodal characteristic vector. The proof for Corollary 1 can be found in the Appendix.

Corollary 1. $-\frac{1}{\sqrt{N(1-p\lambda_1)}}\|\mathbf{y}\| \leq \max(CC) \leq \frac{1}{1-p\lambda_1}\|\mathbf{y}\|$.

3.2 Approximations of Cascade Centrality in the case $p\lambda_1 > 1$

In this section, we consider an approximation for cascade centrality in the particular case that $p\lambda_1 > 1$, which represents the case of viral spread. We have the decomposition for CC

$$CC = \sum_{j=1}^n \sum_{t=0}^T (p\lambda_j)^t U_j U_j^T \mathbf{y}. \quad (4)$$

By Perron-Frobenius Theorem, we have $|\lambda_j| \leq \lambda_1$ for every j . If we furthermore assume that the graph is non-periodic, then in fact $|\lambda_j| < \lambda_1$ for all $j \neq 1$. Note the typical random graph is not periodic, so this assumption is reasonable. Thus the term $(p\lambda_1)^t$ grows exponentially faster than $(p\lambda_j)^t$ for $j \neq 1$, so that the $j = 1$ term dominates for sufficiently large values of T and we obtain the approximation:

$$CC(\mathbf{A}, p, \mathbf{y}, T) \approx CC_{\text{approx}} = \left(\sum_{t=0}^T (p\lambda_1)^t \right) U_1^T \mathbf{y} U_1. \quad (5)$$

Note that in many cases of interest, λ_1 is significantly larger than λ_2 , in which case the above approximation becomes strong even for modest values of T . For example, in Erdos-Reyni graphs $G(n, p)$ with $np \geq c \log(n)$, we have $\lambda_1 = np + O(\sqrt{np})$ whereas $|\lambda_j| = O(\sqrt{np})$ for all $j \neq 1$.

This approximation reveals some nice properties of Cascade Centrality. Crucially, note that CC_{approx} is simply a scalar multiple of the eigenvector U_1 . According to the Perron-Frobenius Theorem, all elements in this eigenvector are positive. Hence, we observe that the expected cascade payoff for seeding any individual is negative under CC_{approx} if $U_1^T \mathbf{y} < 0$. In particular, we can see that the sign of $U_1^T \mathbf{y}$ determines the direction of the relationship between CC_{approx} and eigenvector centrality:

- If $U_1^T \mathbf{y} > 0$, the rankings of nodes in CC_{approx} and eigenvector centrality are the same.
- If $U_1^T \mathbf{y} < 0$, the rankings of nodes in CC_{approx} is in the opposite direction as that in eigenvector centrality.

Note that if $U_1^T \mathbf{y} = 0$, then CC_{approx} is not a good approximation so we disregard this case.

We now relate Cascade Centrality to diffusion centrality ($C_{\text{Diffusion}}$). Diffusion centrality measures the expected number of times a piece of information originating from an individual is heard by other individuals in the network. It can be approximated by $C_{\text{Diffusion}} = \left(\sum_{t=1}^T (p\mathbf{A})^t \right) \mathbf{1} \approx C_{\text{Diffusion}}^{\text{approx}} = \sum_{t=1}^{\infty} (p\lambda_1)^t U_1 (U_1^T \mathbf{1})$.

Since all entries in U_1 are positive, we have $U_1^T \mathbf{1} > 0$, and so $C_{\text{Diffusion}}^{\text{approx}}$ is a positive scalar multiple of U_1 .

We see, as with Eigenvector Centrality, that if $U_1^T \mathbf{y} > 0$, then CC_{approx} scales positively with $C_{\text{Diffusion}}^{\text{approx}}$, whereas if $U_1^T \mathbf{y} < 0$, then CC_{approx} scales negatively with $C_{\text{Diffusion}}^{\text{approx}}$.

It worth mentioning that when $p\lambda_1 < 1$, the approximation CC_{approx} is no longer reliably strong.

3.3 Robustness of Cascade Centrality

Since real-world data is noisy and dynamic, it is essential to analyze the robustness of the centrality measures. In this section, we measured the robustness of Cascade Centrality using the Euclidean norm of the difference between the actual Cascade Centrality and observed Cascade Centrality in the presence of noisy data, $\|\Delta CC\| = \|\tilde{CC} - CC\|$. In particular, we analyze both the imperfect observation of individual influence and the network. In this section, we work under the assumption that $p\lambda_1 < 1$.

Imperfect observation of nodal influence vector \mathbf{y} We now analyze the robustness of Cascade Centrality with imperfect observation of \mathbf{y} . We assume the observed and actual nodal influence are $\hat{\mathbf{y}}$

and \mathbf{y} respectively. The error in the nodal influence vector is $\Delta\mathbf{y} = \mathbf{y} - \hat{\mathbf{y}}$. Given the noise, we can write ΔCC as

$$\Delta CC = \sum_{t=0}^T (p\mathbf{A})^t \Delta\mathbf{y} = \mathbf{U} \sum_{t=0}^T (p\mathbf{\Lambda})^t \mathbf{U}^T \Delta\mathbf{y}. \quad (6)$$

The bounds for $\|\Delta CC\|$ show the robustness of the Cascade Centrality for a particular network. The bounds for the Euclidean norm of ΔCC are shown in Eq.(7). In general, the larger the $p\lambda_1$, the less robustness the Cascade Centrality. Moreover, unsurprisingly, the larger the Euclidean norm of the error, the less robustness the Cascade Centrality.

$$1 + p\lambda_n \|\Delta\mathbf{y}\| \leq \|\Delta CC\| \leq \sum_{t=0}^T (p\lambda_1)^t \|\Delta\mathbf{y}\| \leq \frac{1}{1 - p\lambda_1} \|\Delta\mathbf{y}\|. \quad (7)$$

Imperfect observation of the network \mathbf{A} We analyze the robustness of CC with an imperfect observation of the network. We assume the imperfect observation and the real network as \mathbf{A} and $\hat{\mathbf{A}}$. Let $\Delta\mathbf{A} = \mathbf{A} - \hat{\mathbf{A}}$, we obtain the Corollary 2 with the proof shown in Appendix.

Corollary 2. *When $\Delta\mathbf{A}$ is sufficiently small such that $p(\rho(\hat{\mathbf{A}}) + \rho(\Delta\mathbf{A})) < 1$,*

$$\|\Delta CC\| \leq \frac{1}{1 - p(\rho(\hat{\mathbf{A}}) + \rho(\Delta\mathbf{A}))} - \frac{1}{1 - p\rho(\hat{\mathbf{A}})} \quad (8)$$

4 Cascade Centrality with noisy observations

In the previous section, we analyze the robustness of CC when either nodal influence vector or the network is imperfectly observed. Noises widely exist in the real world. However, there is a lack of study in simultaneously estimating both the network and the nodal influence vector.

To solve this challenge, we take advantage of homophily, a long-standing phenomenon in social networks that interest researchers in social science and economics. It has been widely confirmed that people's ego-networks are homogeneous about many social-demographics, behavioral and intra-personal characteristics [21, 11, 14]. Therefore, we utilize the fact that the distribution of nodal influence on the network reveals information about the network structure to help with the inference. To this end, we formulate a joint optimization problem to collectively uncover the observed nodal influence vector and networks with a joint optimization from noisy data.

4.1 Problem formulation

Given the observed noisy observations on the network and the nodal influence vector, we want to estimate the actual network and nodal influence to more accurate Cascade Centrality. The homophily in nodal evaluations presented in the network is quantified by the Laplacian quadratic form $\mathbf{y}^T \mathbf{L} \mathbf{y}$, which smooths the distribution of influence vector across the network. The quadratic form encourages the smoothness of the nodal influence with respect to the corresponding network. In particular, the smaller this quadratic form, the more similar the nodal influence among neighbors. We impose a regularization term on the adjacency matrix to avoid the over-complexity of the network. In particular, we control the distribution of the the Frobenius norm of off-diagonal entries in the adjacency matrix. Up to this point, we propose the following joint optimization in Eq.(9). The first two terms to minimize the differences between the inferred and observed network, as well as the inferred and observed influence vector.

$$\begin{aligned} \text{minimize}_{\mathbf{A}, \mathbf{y}} \quad & f(\mathbf{A}, \mathbf{y}) = \frac{1}{2} \|\mathbf{A} - \hat{\mathbf{A}}\|_F^2 + \theta_1 \frac{1}{2} \|\mathbf{y} - \hat{\mathbf{y}}\|_F^2 + \theta_2 (\mathbf{y}^T \mathbf{L} \mathbf{y}) + \theta_3 \frac{1}{2} \|\mathbf{A}\|_F^2 \\ \text{subject to} \quad & A_{ij} = A_{ji}, A_{ij} \geq 0, i \neq j, \\ & A_{ii} = 0, \end{aligned} \quad (9)$$

where $\hat{\mathbf{A}}$ and $\hat{\mathbf{y}}$ are the observed social network and the nodal influence vector. θ_1 controls the relative importance in matching \mathbf{y} versus matching \mathbf{A} with the real data. θ_2 and θ_3 are the regularization

parameters controlling the strength of homophily and the regularization of the network. The other remaining constraints guarantee that the learned \mathbf{A} is a valid adjacency matrix.

4.2 Learning algorithm

Since the optimization function is not joint convex in \mathbf{A} and \mathbf{y} , we use an iterative approach which alternatively optimizes over \mathbf{y} and \mathbf{A} . Given the inference for \mathbf{y} , we solve for Eq.(9) to estimate \mathbf{A} . Similarly, fixing \mathbf{A} , we estimate \mathbf{y} . We repeat this process until the convergence criterion is reached. We summarize our de-noising algorithm in Algorithm 1. And we next discuss each update step in details.

Algorithm 1 De-noising algorithm for computing CC .

- 1: **Input** Observed network $\hat{\mathbf{A}}$, observed nodal influence vector $\hat{\mathbf{y}}$, θ_1 , θ_2 and θ_3 .
 - 2: **Output** $\mathbf{A} \in \mathbb{R}^{N \times N}$, influence vector $\mathbf{y} \in \mathbb{R}^{N \times 1}$, and CC .
 - 3: **Initialize** $\mathbf{A}_0 = \hat{\mathbf{A}}$, $\mathbf{y}_0 = \hat{\mathbf{y}}$, $t = 1$
 - 4: **while** $\Delta \geq 10^{-4}$ and $t \leq \#$ iterations **do**
 - 5: Solve for \mathbf{A}_t with Eq.(9) given \mathbf{y}_{t-1} .
 - 6: Update \mathbf{y} with Eq.(14) given \mathbf{A}_t
 - 7: $\Delta = f(\mathbf{A}_t, \mathbf{y}_t) - f(\mathbf{A}_{t-1}, \mathbf{y}_{t-1})$
 - 8: $t = t + 1$
 - 9: **end while**
 - 10: Compute CC by plugging $\mathbf{A} = \mathbf{A}_{\text{iter}}$ and $\mathbf{y} = \mathbf{y}_{\text{iter}}$ into Eq.(2).
-

Update \mathbf{A} We use a partial-gradient based approach to solve for \mathbf{A} given \mathbf{y} . We use first-order partial derivative of \mathbf{A} for updating and second-order partial derivative to show that this problem is convex. The first-order derivative of the objective function with respect to \mathbf{A} is,

$$\frac{\partial f(\mathbf{A}, \mathbf{y})}{\partial \mathbf{A}} = (\mathbf{A} - \hat{\mathbf{A}}) + \theta_3 \mathbf{A} + g(\mathbf{y}), \quad (10)$$

where $g(\cdot)$ is a function of \mathbf{y} , which vanishes in the second-order derivative,

$$\frac{\partial f(\mathbf{A}, \mathbf{y})}{\partial^2 \mathbf{A}} = (1 + \theta_3) \mathbf{I}, \quad (11)$$

where \mathbf{I} is an identity matrix. With determinant of Hessian matrix of $f(\mathbf{A}, \mathbf{y})$, $\det(1 + \theta_3 + \lambda) \mathbf{I}$, being positive, $f(\mathbf{A}, \mathbf{y})$ is convex with respect to \mathbf{A} .

Update \mathbf{y} We show that we have a closed-form solution for \mathbf{y} by setting the first-order partial derivative of $f(\mathbf{A}, \mathbf{y})$ over \mathbf{y}_i to be zero. And we use the second-order partial gradient to show that the subproblem is convex. The first-order and second-order partial derivative of $f(\mathbf{A}, \mathbf{y})$ over \mathbf{y}_i are,

$$\frac{\partial f(\mathbf{A}, \mathbf{y})}{\partial \mathbf{y}_i} = \theta_1 (\mathbf{y}_i - \hat{\mathbf{y}}_i) + \theta_2 (\mathbf{L} + \mathbf{L}^T) \mathbf{y}_i = \theta_1 (\mathbf{y}_i - \hat{\mathbf{y}}_i) + 2\theta_2 \mathbf{L} \mathbf{y}_i, \quad (12)$$

and

$$\frac{\partial f(\mathbf{A}, \mathbf{y})}{\partial^2 \mathbf{y}_i} = \theta_1 + 2\theta_2 \sum_{j=1}^N L_{ji}. \quad (13)$$

Setting Eq.(12) to zero, we obtain the closed-form solution for \mathbf{y} condition on \mathbf{A} ,

$$\mathbf{y} = \left(\mathbf{I} + 2 \frac{\theta_2}{\theta_1} \mathbf{L} \right)^{-1} \hat{\mathbf{y}}. \quad (14)$$

With $\sum_{j=1}^N L_{ji} = d_i$, $\theta_1, \theta_2 \geq 0$, we have $\frac{\partial f(\mathbf{A}, \mathbf{y})}{\partial^2 \mathbf{y}_i} \geq 0$. Thus, Eq.(14) guarantees a global minimum of \mathbf{y} given \mathbf{A} .

The algorithm does not guarantee a global minimum since the objective function is not joint convex in \mathbf{A} and \mathbf{y} . However, the iterative algorithm assures a local minimum. In each iteration, the objective function in Eq.(9) always decreases due to the reason that $f(\mathbf{A}, \mathbf{y})$ is convex in one variable by fixing another. In the objective function, the Frobenius norm is no less than 0, and $\mathbf{y}^T \mathbf{L} \mathbf{y} > 0$. Therefore, Eq.(9) has a loose lower bound of 0. Hence, a local minimum is guaranteed with the algorithm.

5 Experiment

In this section, we analyze the performance of Cascade Centrality in selecting individuals to generate payoff and evaluate the de-noise algorithm in inferring the actual network and the nodal influence vector. In particular, we first evaluate Cascade Centrality and the existing widely-adopted centrality measures on Stochastic Block Model based on a variety of synthetic network and three real-world social networks. Then we compare Cascade Centrality computed with our learning algorithm with merely using the observed data.

Synthetic data generation We generate the synthetic data with two equally-sized block, each generated from three types of networks Erdős-Rényi ($p = 0.2$), Barabasi-Albert ($m = 1$) and Watts-Strogatz network ($k = \log_2(N)$, $p = 0.2$) with $N = 500$ nodes. The nodal influence vector of the two blocks $\mathbf{y} \sim \mathcal{N}(\mathbf{1}, 0.1\mathbf{I})$ and $y \sim \mathcal{N}(-1, 0.1\mathbf{I})$ respectively. The diffusion probability is set to be 0.2. And T is set to be the diameter of the graph.

Real-world data We use three real-world datasets to validate our methods. The first one is Zachary’s karate club, which contains a friendships network of 34 members and 78 connections at a US university in the 1970s¹. Second, we select a social network in an Indian village with 107 individuals and 365 links in the mouth-to-mouth marketing of micro-finance². Third, we choose a dense network from the US Airlines with 332 airports and 2461 connections³. We generate the nodal influence vector with a Multi-Variate Normal distribution $\mathcal{N}(\mathbf{0}, \mathbf{L}^{-1})$, where the covariance is the inverse of the ground-truth Laplacian matrix. Similarly, the diffusion probability is set to be 0.2. Moreover, T is set to be the diameter of the graph.

Performance of Cascade Centrality We compare the cascade payoff by seeding with Cascade Centrality, degree centrality, eigenvector centrality, Katz centrality (the attenuation factor set to be $1/\lambda_1 + 0.01$) and diffusion centrality. We also compute the scaled version of these centrality measures by $U_1 \mathbf{y}$. In particular, if the largest of scaled centrality measures or Cascade Centrality is negative, we do not seed any individual. As for the evaluation, we compare the payoff of the cascade by seeding one individual according to a particular centrality. We show our centrality measure in Figure 1. We see that Cascade Centrality outperforms existing centralities. Moreover, with the scaling factor, we improve existing centrality measures in avoiding generating negative cascade payoffs. When the network is very dense as in the US-Airline network, our centrality measure has limited improvement since nodes with positive and negative influence are well mixed.

Performance of the de-noise algorithm To evaluate the performance of our algorithm in a noisy environment, we perturb the nodal influence vector and the network with zero-mean Gaussian random noise. We then evaluate the correlation between the observed or the de-noised Cascade Centrality from our method with the actual Cascade Centrality from the true data. We compute the change in the correlation with the Cascade Centrality from the real data by computing Cascade Centrality from the de-noised network and nodal influence vector rather than from the observed data. We present the average payoff generated by the cascade in Figure 2, which shows that with our de-noise algorithm, we can better recover the true Cascade Centrality from both synthetic and real-world data.

6 Conclusion

In this paper, we propose Cascade Centrality to measure the power of individual nodes in generating cascade payoffs. Cascade Centrality nests degree, eigenvector, Katz, and diffusion centrality. Moreover, when the $p\lambda_1 > 1$, the joint distribution of eigenvector and nodal influence vector ($U_1 \mathbf{y}$) controls the sign of cascade payoff, and several existing centrality measures are well-estimated by

¹Data accessed from <http://www-personal.umich.edu/~mejn/netdata/>

²Data accessed from <https://economics.mit.edu/faculty/eduflo/social>. Village 4 has been used.

³Data accessed from <http://vlado.fmf.uni-lj.si/pub/networks/data/mix/usair97.net>

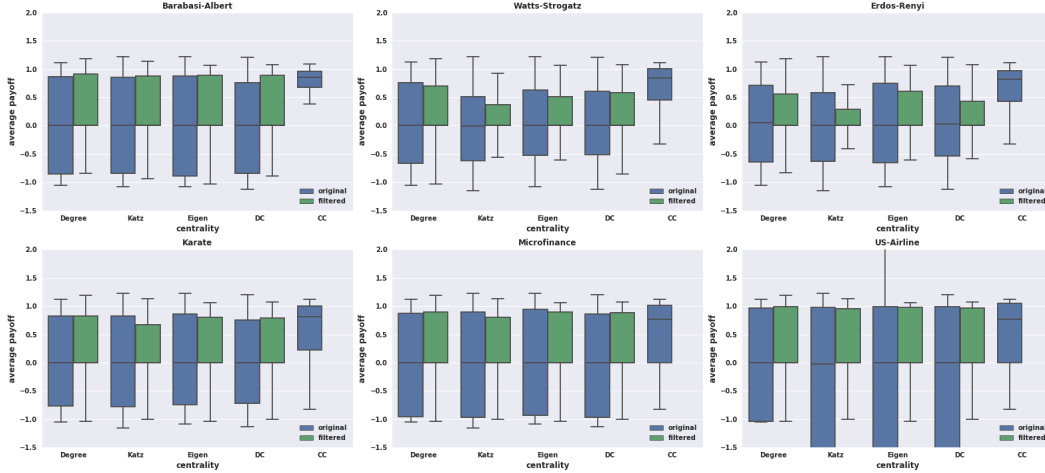


Figure 1: Comparing cascade payoffs by seeding with different centrality measures. The axis shows degree, Katz, eigenvector, diffusion centrality and Cascade Centrality. The blue and green boxplot show the distribution of average payoff and the average payoff when $U_1 \lambda_1 > 0$ in 500 simulations respectively. The lower, median and upper bars in the boxes show 25, 50 and 75 percentile.

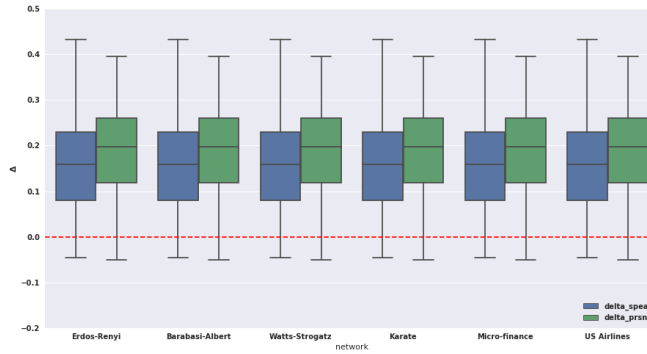


Figure 2: Comparing CC using de-noising algorithm and with the observed data. $\Delta = \text{corr}(CC_{\text{de-noised}}, CC_{\text{actual}}) - \text{corr}(CC_{\text{observed}}, CC_{\text{actual}})$. $\text{corr}(\cdot)$ represents either Spearman or Pearson correlation in green and blue boxes respectively. The red dash line is the reference where the de-noising algorithm has the same performance as simply using the observations.

Cascade Centrality with a scaling factor. To ensure the practical application of Cascade Centrality with noisy measurements, we take advantage of the presence of homophily in a network and formulate a learning problem to simultaneously correct for the noise in nodal characteristic and the network. With experiments on synthetic and real data, we show that Cascade Centrality out-performs existing centrality measures in generating cascade payoffs. Moreover, with the multiplier mentioned above, we can avoid the negative payoffs with existing centralities. Lastly, we show that after de-noising with our algorithm, we can better proxy the actual Cascade Centrality than simply using observations.

Our study points out several directions for future work including 1) factoring in nodal influence vector in influence maximization where monotone and submodular properties no longer holds; 2) systematic analysis of the robustness of centrality measures with different types of noises; 3) combining matrix completion and graph learning for more sophisticated methods in estimating nodal influence vector and network structure simultaneously after our first attempt.

References

- [1] Daron Acemoglu, Asuman Ozdaglar, and Alireza Tahbaz-Salehi. Systemic risk and stability in financial networks. *American Economic Review*, 105(2):564–608, 2015.
- [2] Jonathan Aizen, Daniel Huttenlocher, Jon Kleinberg, and Antal Novak. Traffic-based feedback on the web. *Proceedings of the National Academy of Sciences*, 101(suppl 1):5254–5260, 2004.
- [3] Mohammad Taha Bahadori, Qi Rose Yu, and Yan Liu. Fast multivariate spatio-temporal analysis via low rank tensor learning. In *Advances in neural information processing systems*, pages 3491–3499, 2014.
- [4] Coralio Ballester, Antoni Calvó-Armengol, and Yves Zenou. Who’s who in networks. wanted: The key player. *Econometrica*, 74(5):1403–1417, 2006.
- [5] Abhijit Banerjee, Arun G Chandrasekhar, Esther Duflo, and Matthew O Jackson. The diffusion of microfinance. *Science*, 341(6144):1236498, 2013.
- [6] Abhijit Banerjee, Arun G Chandrasekhar, Esther Duflo, and Matthew O Jackson. Gossip: Identifying central individuals in a social network. Technical report, National Bureau of Economic Research, 2014.
- [7] Francis Bloch, Matthew O Jackson, and Pietro Tebaldi. Centrality measures in networks. 2017.
- [8] John W Byers, Michael Mitzenmacher, and Georgios Zervas. The groupon effect on yelp ratings: a root cause analysis. In *Proceedings of the 13th ACM conference on electronic commerce*, pages 248–265. ACM, 2012.
- [9] Nicholas A Christakis and James H Fowler. Social network sensors for early detection of contagious outbreaks. *PloS one*, 5(9):e12948, 2010.
- [10] Andrea Galeotti, Benjamin Golub, and Sanjeev Goyal. Targeting interventions in networks. *arXiv preprint arXiv:1710.06026*, 2017.
- [11] Benjamin Golub and Matthew O Jackson. How homophily affects the speed of learning and best-response dynamics. *The Quarterly Journal of Economics*, 127(3):1287–1338, 2012.
- [12] Roger Guimerà and Marta Sales-Pardo. Missing and spurious interactions and the reconstruction of complex networks. *Proceedings of the National Academy of Sciences*, 106(52):22073–22078, 2009.
- [13] Rishabh K Iyer and Jeff A Bilmes. Submodular optimization with submodular cover and submodular knapsack constraints. In *Advances in Neural Information Processing Systems*, pages 2436–2444, 2013.
- [14] Matthew O Jackson. *Social and economic networks*. Princeton university press, 2010.
- [15] David Kempe, Jon Kleinberg, and Éva Tardos. Maximizing the spread of influence through a social network. In *Proceedings of the ninth ACM SIGKDD international conference on Knowledge discovery and data mining*, pages 137–146. ACM, 2003.
- [16] Justin T Khim, Varun Jog, and Po-Ling Loh. Computing and maximizing influence in linear threshold and triggering models. In *Advances in Neural Information Processing Systems*, pages 4538–4546, 2016.
- [17] Balázs Kovács and Amanda J Sharkey. The paradox of publicity: How awards can negatively affect the evaluation of quality. *Administrative Science Quarterly*, 59(1):1–33, 2014.
- [18] Ernest Liu. Industrial policies and economic development. 2017.
- [19] Jian-Guo Liu, Jian-Hong Lin, Qiang Guo, and Tao Zhou. Locating influential nodes via dynamics-sensitive centrality. *Scientific reports*, 6:21380, 2016.
- [20] Christopher Lynn and Daniel D Lee. Maximizing influence in an ising network: A mean-field optimal solution. In *Advances in Neural Information Processing Systems*, pages 2495–2503, 2016.
- [21] Miller McPherson, Lynn Smith-Lovin, and James M Cook. Birds of a feather: Homophily in social networks. *Annual review of sociology*, 27(1):415–444, 2001.
- [22] Nikhil Rao, Hsiang-Fu Yu, Pradeep K Ravikumar, and Inderjit S Dhillon. Collaborative filtering with graph information: Consistency and scalable methods. In *Advances in neural information processing systems*, pages 2107–2115, 2015.
- [23] Zheng Wen, Branislav Kveton, Michal Valko, and Sharan Vaswani. Online influence maximization under independent cascade model with semi-bandit feedback. In *Advances in Neural Information Processing Systems*, pages 3026–3036, 2017.

Appendix

Proof for Theorem 1

Proof. With Singular Value Decomposition, we can write CC as,

$$CC(\mathbf{A}; p, \mathbf{y}, T) := \sum_{t=0}^T (p\mathbf{A})^t \mathbf{y} = \sum_{t=0}^T (p\mathbf{U}\mathbf{\Sigma}\mathbf{U}^T)^t \mathbf{y} = \mathbf{U} \sum_{t=0}^T (p\mathbf{\Sigma})^t \mathbf{U}^T \mathbf{y} \quad (15)$$

Note that, if we write $\mathbf{y} = \sum_{j=1}^n c_j \mathbf{u}_j$, where \mathbf{u}_j is an orthonormal basis of eigenvectors, then

$$CC(\mathbf{A}; p, \mathbf{y}, T) = \sum_{j=1}^n c_j \sum_{t=0}^T (p\lambda_j)^t \mathbf{u}_j \quad (16)$$

moreover, so, since \mathbf{u}_j is an orthogonal basis, we have

$$\|CC(\mathbf{A}; p, \mathbf{y}, T)\| = \sqrt{\sum_{j=1}^n (c_j \sum_{t=0}^T (p\lambda_j)^t)^2} \quad (17)$$

We note that for each j , under the assumption that $p\lambda_1 < 1$, we can obtain the following bounds: $1 + p\lambda_n \leq \sum_{t=0}^T (p\lambda_j)^t \leq \frac{1}{1-p\lambda_1}$

Plugging these bounds into the above equation, and using the fact that $\sqrt{\sum_{j=0}^n c_j^2} = \|\mathbf{y}\|$, we obtain bounds for the norm of CC :

$$(1 + p\lambda_n)\|\mathbf{y}\| \leq \|CC(\mathbf{A}; p, \mathbf{y}, T)\| \leq \sum_{t=0}^T (p\lambda_1)^t \|\mathbf{y}\| \leq \frac{1}{1-p\lambda_1} \|\mathbf{y}\| \quad (18)$$

□

Proof for Collorary 1

Proof.

$$\max(CC) \leq \|CC\|_2 \leq \frac{1}{1-p\lambda_1} \|\mathbf{y}\|_2 \quad (19)$$

Similarly, we obtain the lower bound for $\max(CC)$. We have

$$\max(CC) \geq -\frac{1}{\sqrt{N}(1-p\lambda_1)} \|\mathbf{y}\| \quad (20)$$

Since if $\max(CC) < -\frac{1}{\sqrt{N}(1-p\lambda_1)} \|\mathbf{y}\|$, that would imply $\|CC\|_\infty > \frac{1}{\sqrt{N}(1-p\lambda_1)} \|\mathbf{y}\|$, hence $\|CC\|_2 \geq \sqrt{N}\|CC\|_\infty > \frac{1}{(1-p\lambda_1)} \|\mathbf{y}\|$, contradicting Theorem 1.

□

Proof for Collorary 2

Proof. Next, we present the proof for Collorary 2 We have $\|\Delta CC\| = \|(\sum_{t=0}^T (p\mathbf{A})^t - \sum_{t=0}^T (p\hat{\mathbf{A}})^t) \mathbf{y}\| \leq \rho(\sum_{t=0}^T (p\mathbf{A})^t - \sum_{t=0}^T (p\hat{\mathbf{A}})^t) \|\mathbf{y}\|$, where $\rho(\cdot)$ is spectral norm of a matrix.

But note that $\rho(\sum_{t=0}^T (p\mathbf{A})^t - \sum_{t=0}^T (p\hat{\mathbf{A}})^t) \leq \rho(\sum_{t=0}^T (p\mathbf{A})^t) - \rho(\sum_{t=0}^T (p\hat{\mathbf{A}})^t)$, since $\rho(\cdot)$ is a norm. Finally, we note that $\rho(\sum_{t=0}^T (p\hat{\mathbf{A}})^t) = \sum_{t=0}^T (p\rho(\hat{\mathbf{A}}))^t$ and similarly $\rho(\sum_{t=0}^T (p\mathbf{A})^t) = \sum_{t=0}^T (p\rho(\mathbf{A}))^t \leq \sum_{t=0}^T (p(\rho(\hat{\mathbf{A}}) + \rho(\Delta\mathbf{A})))^t$. We obtain that

$$\|\Delta CC\| \leq \sum_{t=0}^T (p(\rho(\hat{\mathbf{A}}) + \rho(\Delta\mathbf{A})))^t - \sum_{t=0}^T (p\rho(\hat{\mathbf{A}}))^t \quad (21)$$

If we have $p(\rho(\hat{\mathbf{A}}) + \rho(\Delta\mathbf{A})) < 1$, then we obtain a simplified bound by replacing the above geometric series by convergent infinite series:

$$\|\Delta CC\| \leq \frac{1}{1 - p(\rho(\hat{\mathbf{A}}) + \rho(\Delta\mathbf{A}))} - \frac{1}{1 - p\rho(\hat{\mathbf{A}})} \quad (22)$$

This can be interpreted as a robustness result for CC , given that $\Delta\mathbf{A}$ is sufficiently small, namely small enough that $p(\rho(\hat{\mathbf{A}}) + \rho(\Delta\mathbf{A})) < 1$.

□